

# Ador-Solid-Set: A coupled simulation model for commercial solid-set irrigated fields

Enrique Playán<sup>1</sup> ✉, Nery Zapata<sup>1</sup>, Borja Latorre<sup>1</sup>, José Caverro<sup>1</sup>, Piluca Paniagua<sup>1</sup>,  
Eva T. Medina<sup>1</sup>, María Angeles Lorenzo<sup>2</sup> and Javier Burguete<sup>1</sup>

## **Abstract**

The last five decades have seen strong developments in surface, drip and sprinkler irrigation modeling. However, most of these efforts have targeted irrigation units smaller than a field. In sprinkler irrigation, models have generally been applied to a few sprinklers in a regular arrangement, making them representative of a sector or a whole field. In this research, the Ador-Solid-Set model is presented for whole-field sprinkler irrigation in commercial fields. The model couples pipeline hydraulics, sprinkler ballistics and irrigation scheduling at execution time, permitting to simulate scenarios with minimum data management burden. Field experiments have been used to validate the model in an experimental solid-set. Observed and simulated irrigation depths and coefficients of uniformity showed statistically significant agreement. The model was applied to simulate irrigation events in two commercial solid-sets of 10.2 and 24.5 ha, producing maps of applied water in a sequential irrigation of their irrigation sectors lasting for 24 hours. The solid-set model produced whole-field irrigation performance estimates. The current adequacy thresholds for sprinkler irrigation uniformity need to be revised to apply them to complete solid-sets. The model highlighted the importance of finding suitable combinations of full- and partial-circle sprinklers to achieve optimal performance indicators. Finally, Ador-Solid-Set quantified the volume of drift outside the computational domain. This drift adds to the drift and evaporation losses obtained from empirical equations, in a process that requires further analysis. Research efforts are needed to enhance the current

---

<sup>1</sup> Dept. of Soil and Water, EEAD-CSIC, Avda Montañana 1005, 50059 Zaragoza, Spain.

<sup>2</sup> Dept. Environment, Agricultural and Forest Systems. Associated Unit to EEAD-CSIC, Centro de Investigación y Tecnología Agroalimentaria de Aragón (CITA-Aragón), Gobierno de Aragón, Avda. Montañana 930, 50059 Zaragoza, Spain.

29 model capabilities to address the challenges related to water quantity and quality  
30 in sprinkler solid-sets.

31 **Keywords:** irrigation uniformity; irrigation scheduling; pipeline roughness;  
32 ballistics

### 33 1. Introduction

34 Computer modeling has been an area of growing interest in the past decades.  
35 Modeling has been applied to a wide variety of objects and processes. Interest in  
36 irrigation system models started in the 1970s, with the first modelling applications  
37 being to farm water management (Windsor and Chow, 1971). Models have proven  
38 very useful in irrigation practice, complementing and even partially replacing  
39 irrigation evaluations and experimentation. Computer models permit to quickly  
40 respond to a variety of “what if” questions. In the absence of computer models,  
41 answering these questions would require intense and expensive  
42 experimentation. A large number of models of different types have been  
43 developed for surface, drip and sprinkler systems.

44 The modeling of surface irrigation events has been an active area of research  
45 since the 1970s (Bassett, 1972). The complexity of surface irrigation hydraulics and  
46 the low number of parameters involved in the governing equations accelerated  
47 the adoption of modeling for surface irrigation design, analysis and parameter  
48 estimation. Most surface irrigation models focus on one irrigation unit (a border,  
49 basin or furrow). Only a few of these models focus on surface irrigated fields  
50 (composed of multiple irrigation units), concentrating on issues like the water  
51 distribution network (Pereira et al., 1998) or field-level efficiency (Zapata et al.,  
52 2000). Surface irrigation models have also been applied to simulate water flows in  
53 water users associations (Playán et al., 2000). These models are computationally  
54 intense, since they use numerical methods to solve the shallow-water equations.  
55 One-dimensional simulations were time-consuming in the 1980s. Developments  
56 in numerical techniques and personal computers have made WinSRFR (Bautista  
57 and Schlegel, 2020) - the current standard on 1D surface irrigation simulation - a  
58 fast model. However, two-dimensional models still represent an intense  
59 computational effort.

60 Simulation of drip irrigation also started in the 1970s, and developed in parallel  
61 with the consolidation of this irrigation method. Modeling focused on two different  
62 aspects: pipeline design considering emitter hydraulics and field layout (Wu and  
63 Gitlin, 1974), and the interaction between the emitted water and the soil profile,  
64 following a soil physics approach (Skaggs et al., 2004). The field approach has  
65 been more used in drip irrigation than in surface irrigation, responding to the need  
66 for whole-field design in conditions of almost continue water delivery along the  
67 emitter lines.

68 Sprinkler irrigation modeling started almost a decade later than surface and drip  
69 irrigation modeling. Fukui et al., (1980) presented a ballistic sprinkler irrigation  
70 model that laid down the basic structure of current models. A number of  
71 improvements to the original model were performed (Carrión et al., 2001; Montero  
72 et al., 2001; Seginer et al., 1991; Vories et al., 1987). As a result, by the beginning of  
73 the 21<sup>st</sup> century, sprinkler irrigation models were functional in field conditions and  
74 could be calibrated with experimental data. Ballistic models have been applied to  
75 solid-sets (Ador-Sprinkler) (Playán et al., 2006) and moving laterals (Ouazaa et  
76 al., 2015). While the models for moving laterals typically implement all the emitters  
77 in a sprinkler irrigated field, solid-set fields have been typically represented by a  
78 short number of full-circle sprinklers distributed in a given spacing and operating  
79 at the same pressure (Dechmi et al., 2003). When attempting to simulate the  
80 sectors in which a solid-set field is typically divided, a number of sprinklers have  
81 been used to reproduce each sector (Zapata et al., 2017). This approach has been  
82 used in Ador- simulation to model the performance of solid-sets, moving laterals  
83 and drip irrigated fields connected to a collective pressurized network (Zapata et  
84 al., 2023). These models have been connected to soil – water – yield models, such  
85 as Ador-Crop (Dechmi et al., 2004), to generate irrigation demand and to estimate  
86 crop yield and soil water content under different structural and water  
87 management scenarios.

88 Despite the success obtained when simulating solid-sets in large irrigated areas  
89 supplied by pressurized networks, the simplifications behind these models are  
90 relevant. In real life solid-sets, sprinklers are not always separated by the exact  
91 nominal spacing. This may be due to problems in construction (unlikely in these

92 days, since GPS systems are used) or to the limitations imposed by the field  
93 dimensions or shape. Additionally, all sprinklers operate at different pressures.  
94 Moreover, two types of impact sprinklers are present in solid-sets: full-circle and  
95 partial-circle. Preparing for the future development of field-scale solid-set  
96 models, Ouazaa et al. (2016) performed experiments to characterize different  
97 types of sprinklers used at the field boundaries, and parametrized a ballistic model  
98 to reproduce their patterns of water application. In a further effort, Robles et al.  
99 (2019) developed a self-calibrated ballistic model for impact sprinklers, based on  
100 a database containing the results of the experiments required to calibrate a given  
101 combination of sprinkler model and nozzle diameter(s). These tests typically  
102 include the determination of the radial application pattern of an isolated sprinkler  
103 under no wind conditions and the determination of the water application pattern in  
104 a catch can network within a sprinkler spacing at different wind speeds. All these  
105 experiments are performed at a range of operating pressures, typically in the  
106 range of 200 - 400 kPa. In order to prevent poor overlap in the presence of high  
107 wind speeds, at least 16 sprinklers are used in these tests, with 25 catch cans being  
108 located in the central spacing (5 x 5 in a square arrangement). The combination of  
109 experiments with different sprinkler types (full-cycle and partial cycle) and  
110 pressures, in isolated sprinklers and in groups of sprinklers sets the scene for the  
111 development of solid-set models at the field scale.

112 In our experience, solid-sets often have a triangular 18 x 18 m sprinkler spacing  
113 and irrigate an area that usually extends from 1 ha to about 40 ha. Fields with  
114 shapes approximating a full circle or a partial circle and with areas in excess of 20  
115 ha are often irrigated with center pivots. These machines have relevant  
116 advantages over solid-sets: cost-effectiveness, high uniformity with low wind  
117 effects and ease to mechanize farming operations. In many areas of the world,  
118 such large fields are not frequent and thus solid-sets are common. The simulation  
119 of water flows in a solid-set is characterized by the complexity of its layout.

120 De Andrade et al. (1999b, 1999a) and de Andrade and Allen (1999) presented the  
121 SPRINKMOD model, which simulates pressure along sprinkler irrigation  
122 distribution networks and flow through the sprinklers. The model did not simulate  
123 the distribution of water applied to the field surface, but solved flow in all pipelines.

124 With these features, SPRINKMOD focused on hydraulic uniformity and on attaining  
125 a minimum value of sprinkler pressure, but could not estimate irrigation  
126 uniformity or efficiency.

127 In the past decades, solid-set irrigation modeling has focused on water  
128 distribution in a sprinkler spacing using ballistics, although hydraulic pipeline  
129 modeling has been applied for decades now, and the combination of pipeline  
130 hydraulics and drop ballistics has already been simulated (Zapata et al., 2017).  
131 Solid-set irrigation models have been used to guide irrigation in small-scale (a  
132 sprinkler spacing) and large-scale applications (a collective pressurized  
133 network). However, the meso scale represented by a solid-set field is particularly  
134 useful to assess farmers' irrigation strategies and to establish relationships  
135 between water application, crop yield and diffuse pollution.

136 In a clear precedent to this work, Morcillo García et al. (2021) presented a model for  
137 solid-set irrigation at the field scale. Their model used EPANET (Rossman et al.,  
138 1994) to simulate flow in the solid-set pipelines and the SIRIAS ballistic model  
139 (Carrión et al., 2001) to simulate water distribution from the sprinkler to the soil  
140 surface. The experimental field was 2,82 ha in area, and was divided in two sectors.  
141 An EPANET layout of the field pipelines was created using the irrigation system  
142 design and a digital terrain model. EPANET was calibrated using pressure sensors  
143 at the sprinklers. Roughness was estimated for the main and submain pipelines,  
144 as well as for the risers. Radial curves were obtained for a full-circle and a partial-  
145 circle sprinkler at different wind speeds. These curves were used in SIRIAS to  
146 produce a database of sprinkler application simulations in the experimental plots  
147 under different pressure and meteorological conditions. These sprinkler  
148 application patterns were overlapped in the SORA software (Montero et al., 2001)  
149 to create a map of water application in the field for each irrigation event. Research  
150 was completed by using simulated water application as input to the AquaCrop  
151 model (Steduto et al., 2009) and comparing yield maps to maps of Normalized  
152 Difference Vegetation Index (NDVI).

153 Barberena et al. (2022) combined QGIS and EPANET to elaborate a model to assess  
154 sprinkler irrigation performance in greenhouses. The model was based on the

155 overlap of individual sprinkler application in windless conditions. An irrigation  
156 design with a number of irrigation sectors was simulated at different pressures.

157 In recent years, the concept of digital twins (Jones et al., 2020) has received  
158 attention by researchers, particularly in the industrial domain. These authors  
159 described digital twins as “a physical entity, a virtual counterpart, and the  
160 connections between them”. This concept, allegedly coined in 2003, can be readily  
161 applied to solid-set fields, using models reproducing their characteristic features  
162 and exploring the connections between the field and the models... probably the  
163 most interesting part. Connections include processes such as irrigation  
164 scheduling, whole-field and whole-season uniformity as related to physical and  
165 meteorological parameters, the dependence on the conditions at the field inlet  
166 (commonly, pressure at the hydrant of a collective pressurized network), the  
167 generation of deep percolation and the diffuse pollution associated to it. The  
168 problems resulting from overfertilization in countries such as Spain, with  
169 escalating animal farming activities leading to abundance of organic fertilizers,  
170 require development of local strategies combining irrigation and fertilization.  
171 Digital twins and simulation models are close concepts. In the context of Agric.  
172 Water Manag, both can provide field-scale strategies alleviating quantitative and  
173 qualitative pressure on water resources.

174 The research group has produced the Ador family of irrigation simulation models  
175 (Dechmi et al., 2004; Playán et al., 2006; Zapata et al., 2023). This paper presents the  
176 development and initial results of a new family member: Ador-Solid-Set, a  
177 simulation model for solid-set sprinkler fields. The model has been conceived as  
178 a tool to identify best practices for agricultural production and the conservation of  
179 irrigation water quantity and quality.

180 The objectives of this research are: 1) to develop Ador-Solid-Set, a coupled model  
181 for whole-field solid-set sprinkler irrigation targeting commercial fields;  
182 pipelines, sprinkler ballistics and irrigation scheduling; 2) to validate the model in  
183 an experimental solid-set; and 3) to apply the model to perform irrigation events  
184 in two commercial solid-sets.

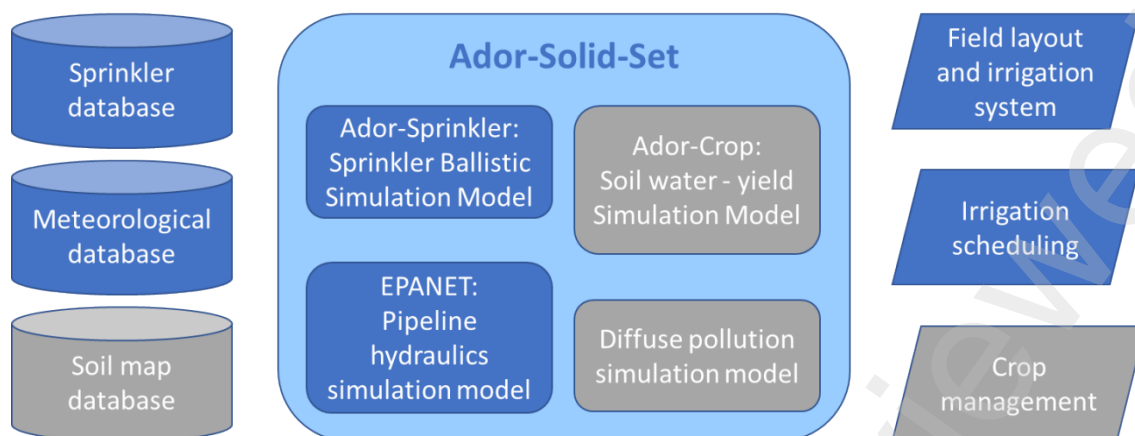
185 **2. Materials and methods**

## 186 2.1. Model concept

187 The main elements of Ador-Solid-Set are presented in Fig. 1. The model currently  
188 consists of a solid-set simulation C++ code coupled to: 1) a new Ador-Sprinkler  
189 release (a ballistic C++ solid-set irrigation model); 2) a C++ meteorological library;  
190 3) a C++ irrigation scheduling library; and 4) EPANET. Previous developments in  
191 Ador-Sprinkler (Playán et al., 2006) have required a major upgrading to move from  
192 a regular, sixteen-sprinkler layout with uniform irrigation material, spacing and  
193 operating pressure to the real, irregular layout of commercial solid-set fields  
194 equipped with full- and partial-circle sprinklers operating at different times and  
195 with different pressures. Coupling Ador-Sprinkler and EPANET at run time has  
196 permitted to determine pressure and discharge conditions in each field sprinkler,  
197 considering the sectors in which the field is divided and the sequential operation  
198 resulting from typical irrigation schedules. Another advantage of this coupling is  
199 that ballistic simulations are performed in any point of the field and at any instant  
200 of simulated time, resulting in water distributions responding to the specific  
201 hydraulic conditions of each sprinkler and to the specific meteorology of each  
202 simulation time step.

203 Simulated water application is delivered to the cells of a square grid. Following the  
204 usual practice in Ador-Simulation, a sprinkler spacing contains about 25 cells of  
205 the square grid. This cell density permits to reveal the variability in water related  
206 properties (yield, uniformity, percolation) at the sprinkler spacing scale. In Ador-  
207 Solid-Set, this variability at the sprinkler spacing scale is combined with the  
208 variability at the field scale. The integration of these sources of variability  
209 represents a relevant step forward in the understanding of solid-set field  
210 performance.

211 Figure 1 presents in blue the current model developments, and in grey the  
212 elements required to complete the model concept. Research is in progress to  
213 integrate these elements and to render Ador-Solid-Set operative to reach its  
214 overall goals.



215

216 **Figure 1.** *Databases (left) submodels (center) and parametrization (right) of the*  
 217 *Ador-Solid-Set model. The parts in grey represent ongoing model developments.*

218 The model can be run for a period of time, typically a natural year. The model time  
 219 step for irrigation application is dictated by the semi hourly availability of  
 220 meteorological data. Air temperature, relative humidity, wind speed, wind  
 221 direction, and solar radiation are available at this time step. Additional variables  
 222 are available at a daily time step: precipitation, maximum and minimum air  
 223 temperature, solar radiation, average relative humidity, average wind speed and  
 224 reference evapotranspiration. These data were obtained from  
 225 agrometeorological stations of Spain via the Agroclimatic Information System for  
 226 Irrigation (SiAR network, Ministry of Agriculture, Fisheries and Food in  
 227 cooperation with the Autonomous Communities).

## 228 2.2. Modelling flow in solid-set pipelines

229 The EPANET software is used to represent the key elements of solid-set  
 230 hydraulics:

- 231 • The hydrant. An elevated reservoir is used for this purpose, assuming that  
 232 solid-set demand does not modify hydrant pressure.
- 233 • Buried pipelines. Represented by the x, y, z coordinates of their extremes,  
 234 their length, diameter and roughness, as well as the pipelines connected in  
 235 the extremes. PVC and Polyethylene are common plastic materials for  
 236 these pipes.
- 237 • Vertical pipelines. These are the sprinkler risers, commonly built in  
 238 galvanized iron and connected to a buried plastic pipeline and a sprinkler.



- 239 • Valves. These are used to open / close sectors. As a consequence, the  
 240 sprinklers located downstream from a sector valve are associated to the  
 241 sector.
- 242 • Emitters or sprinklers. These are represented by a reference, the sprinkler  
 243 coordinates, the connection to a riser pipeline and the k coefficient ( $L s^{-1} m^{-0.5}$ ),  
 244 obtained by dividing the sprinkler discharge  $q$  ( $L s^{-1}$ ) by the square root  
 245 of nozzle pressure  $h$  (m of water column):

$$246 \quad k = c (2g)^{\frac{1}{2}} \pi \frac{1}{4} \left( \frac{D}{1000}^2 + \frac{d}{1000}^2 \right) 1000 \quad [1]$$

247 Where  $c$  is the sprinkler head loss coefficient (0.97 in this research),  $g$  is the  
 248 acceleration of gravity ( $m s^{-2}$ ),  $D$  is the main sprinkler nozzle diameter (mm) and  $d$   
 249 is the auxiliary sprinkler nozzle diameter (mm).

250 The EPANET programming library was included in the Ador-Solid-Set model to  
 251 open and close valves dynamically, responding to an irrigation programming  
 252 schedule. Irrigation simulation starts with a call to the EPANET simulation routine  
 253 to determine - for a given combination of open sectors - the pressure and  
 254 discharge of each operating sprinkler.

### 255 **2.3. Modelling flow from the sprinkler nozzle to the soil surface**

256 The Ador-Sprinkler library has evolved to simulate irrigation in a set of impact  
 257 sprinklers installed within an irregular field perimeter. The parametrization of the  
 258 solid-set field requires the following data:

- 259 • The field perimeter, in  $x, y, z$  coordinates.
- 260 • An additional set of  $x, y, z$  coordinates, used to estimate soil surface  
 261 elevation inside the perimeter.
- 262 • The model and nozzle diameters of each type of sprinkler used in the solid-  
 263 set. Additionally, the corresponding simulation parameters. As described  
 264 by Li et al. (1994), the distribution of diameters of the drops emitted by a  
 265 sprinkler can be represented by a mean drop diameter ( $D_{50}$ , mm) and a  
 266 shape coefficient ( $n$ ). Tarjuelo et al. (1994) developed the relation proposed  
 267 by Seginer et al. (1991), proposing parameters  $K_1$  and  $K_2$ , which determine  
 268 the response of drop trajectories in the presence of wind.

- 269       • A list of the field sprinklers: reference (the same as the one used in  
270           EPANET), type (full or partial circle), x and y coordinates, sprinkler model,  
271           riser height and number of simulated drops in each irrigation event.  
272       • Size of the square computational cells.

273 This information is used by the library to set up the sprinkler objects and to create  
274 a list of the computational cells. Cell properties include:

- 275       • Coordinates x, y, z of the cell center  
276       • Field sector where this cell is located.  
277       • Type of cell:
- 278           ○ External. Completely out of the perimeter. Drops reaching these  
279           cells interrupt their trajectory. Their volume adds to the estimation  
280           of drift.
  - 281           ○ Internal. The cell center is inside the perimeter. When a drop flies  
282           over one of these cells, the calculation of trajectory continues. If the  
283           drop reaches the soil surface, its volume adds to precipitation in the  
284           cell.
  - 285           ○ Internal boundary. A small part of the cell is inside the perimeter,  
286           but the cell center is outside the perimeter. The trajectory is  
287           determined. If the drop reaches the soil surface, its volume adds to  
288           precipitation in the boundary cells (separated from internal cells).
  - 289           ○ External boundary. Located just outside the perimeter, adjacent to  
290           an internal boundary cell. The trajectory is determined. If the drop  
291           reaches the soil surface, its volume adds to the estimation of drift.

292 Robles et al., 2019 presented a detailed description of the determination of  
293 individual drop trajectories in Ador-Sprinkler. The method is based on the  
294 numerical solution of the ballistic governing equations using a third order Runge-  
295 Kutta scheme (Press et al., 1988). The irrigation simulations presented in this  
296 paper were based on the trajectory of 10,000 drops emitted from each sprinkler  
297 (full- or partial-circle). This large number of drops ensures that the volume of  
298 drops landing in each cell is representative of irrigation precipitation.

299 Ador-Sprinkler determines Wind Drift and Evaporation Losses (WDEL) using an  
300 empirical equation derived from all experiments in its data set (Robles et al., 2019).  
301 In this equation, WDEL depends on wind speed, air temperature, relative humidity,  
302 the operating pressure and the main and auxiliary diameter nozzles.

303 The drops landing on external boundary cells or flying above external cells directly  
304 contribute to drift outside the domain. These losses are denoted in the model as  
305 “additional drift”, since WDEL empirical equations are obtained from experiments  
306 in which some drift losses are already included. In WDEL experiments the  
307 experimental sprinkler spacing is surrounded by buffer sprinkler spacings. As a  
308 consequence, in windy conditions, only small drops can be incorporated in the  
309 wind stream and drift away from the experimental area. Large drops drifting in and  
310 out of the experimental sprinkler spacing would compensate, since they can only  
311 drift for small distances. Additional drift can be relevant when the wind blows  
312 irrigation water from partial-circle sprinklers on a field boundary directly out of  
313 the field area.

#### 314 **2.4. Experimental sprinklers and their calibration**

315 Four plastic sprinklers were used in this paper:

- 316 • VYR36 manufactured by VYRSA (Burgos, Spain). This is a full-circle impact  
317 sprinkler with brass nozzles, diameters 4.4 mm and 2.4 mm.
- 318 • VYR66 manufactured by VYRSA (Burgos, Spain). This is a partial-circle  
319 impact sprinkler with brass nozzles, diameters 4.0 mm and 2.4 mm.
- 320 • NDJ 5035 manufactured by NaanDanJain (Jalgaon, India). This is a full-  
321 circle impact sprinkler with plastic nozzles, diameters 4.5 and 2.5 mm.
- 322 • NDJ 5035SD manufactured by NaanDanJain (Jalgaon, India). This is a  
323 partial-circle impact sprinkler with a plastic nozzle, diameter 4.0 mm.

324 All sprinklers were parametrized using two types of experiments. Sprinkler NDJ  
325 5035 was experimentally characterized by Paniagua (2016). The protocol used for  
326 the other three sprinklers is described in the following paragraphs.

327 The first type of experiments featured isolated sprinklers. The experiments for  
328 NDJ 5035 were performed under no-wind conditions at the outdoor facility of  
329 CITA-Aragón, while the experiments for the rest of sprinklers were performed at

330 CENTER, the Central Laboratory for Irrigation Equipment and Materials Testing,  
331 (San Fernando de Henares, Madrid, Ministry of Agriculture, Fisheries and Food,  
332 Government of Spain). Experiments were performed at 200, 300 and 400 kPa,  
333 measuring radial water application at 0.5 m spacing.

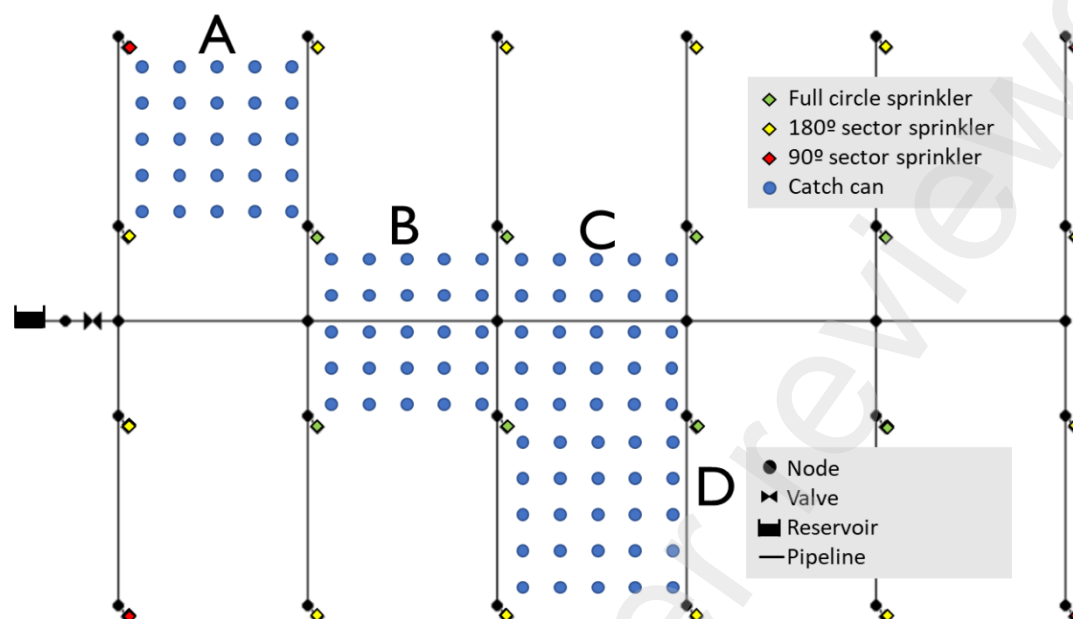
334 The second type of experiments, featuring overlapped sprinklers, was performed  
335 at the outdoor facility of EEAD-CSIC. In partial-circle sprinklers, two sprinklers  
336 irrigating 180° were arranged facing each other, separated by a distance of 18 m.  
337 Fifty catch cans were installed covering the area of 36 x 18 m between both  
338 sprinklers, with a spacing of 3.6 x 3.6 m. In full-circle experiments, a network of 16  
339 sprinklers in a square 18 x 18 m arrangements was used. Twenty-five catch cans  
340 spaced 3.6 x 3.6 m were installed in the central spacing. Experiments were  
341 performed at 200, 300 and 400 kPa and variable wind speeds, with a minimum of  
342 0.48 m s<sup>-1</sup> and a maximum of 4.50 m s<sup>-1</sup>.

343 Sprinkler parameters were determined from these experiments using the  
344 Multiple-Purpose Calibration and Optimization Tool (MPCOTool). This is a free  
345 calibration module that allows estimating the empirical parameters used in  
346 physical models once the objective function is defined (Burguete and Latorre,  
347 2018). When applied to sprinkler parameter estimation, MPCOTool uses a  
348 combination of the Monte-Carlo, hill climbing and iterative method algorithms  
349 (Robles et al., 2019).

## 350 **2.5. Experimental solid-set**

351 An experimental solid-set was installed to validate model performance under  
352 controlled conditions. The solid-set had 24 sprinklers connected to a hydrant of  
353 the pressurized water distribution network of the EEAD-CSIC experimental farm.  
354 Full-circle sprinklers were VYR 36, while partial circle sprinklers were VYR 66. The  
355 field layout in the figure was prepared in EPANET. The figure shows the hydrant  
356 (represented as an elevated reservoir), the valve, the buried pipelines and the  
357 galvanized steel risers (depicted as short diagonal lines connecting the sprinklers  
358 to underground nodes). Four sprinkler spacings were used for experimentation,  
359 containing different types of sprinklers: full-circle and partial-circle (180° and  
360 90°). Each experimental sprinkler spacing was equipped with a network of 5 x 5

361 catch-cans spaced 3.6 x 3.6 m. The main pipeline (horizontal in the Figure) had an  
 362 azimuth of 129°. All sprinklers operated at 300 kPa.



363

364 **Figure 2.** *Outline of the experimental solid-set. The sprinkler, pipeline, reservoir*  
 365 *and valve layout reproduce the EPANET layout. The 25 catch-cans installed in*  
 366 *sprinkler spacings A to D were located at the center of 3.6 x 3.6 m cells laid out*  
 367 *between four sprinklers. Horizontal and vertical pipelines were buried 0.80 m*  
 368 *deep. Short, diagonal pipelines represent the vertical sprinkler risers, running*  
 369 *from 0.80 m below soil surface to 2.25 m above soil surface. The sprinkler spacing*  
 370 *was square, 18 m in side.*

371 Three irrigation events were performed in the experimental solid-set (Table 1).  
 372 Meteorological data were recorded at 30 min intervals and averaged for the Table.  
 373 Vector averaging was used for wind speed/direction. Every irrigation event was  
 374 reproduced as a succession of 30 min simulations, accumulating the precipitation  
 375 received in each computational cell (coincident with each catch can). Observed  
 376 and simulated precipitation in each catch-can and observed and simulated  
 377 Coefficients of Uniformity (Christiansen, 1942) in each sprinkler spacing were  
 378 compared to assess the predictive capacity of the model.

379 **Table 1.** *Duration and average meteorological variables of the three irrigation*  
 380 *events in the experimental data set.*

Experiment	Duration (hours)	Air Temperature	Relative Humidity	Wind Speed	Wind Direction
------------	---------------------	--------------------	----------------------	---------------	-------------------

		(°C)	(%)	ms <sup>-1</sup>	(°)
VYR1	2.5	13.5	64.4	0.780	179
VYR2	3.0	18.4	45.5	0.253	176
VYR3	3.0	17.1	37.7	2.964	118

381

## 382 2.6. Commercial solid-set fields

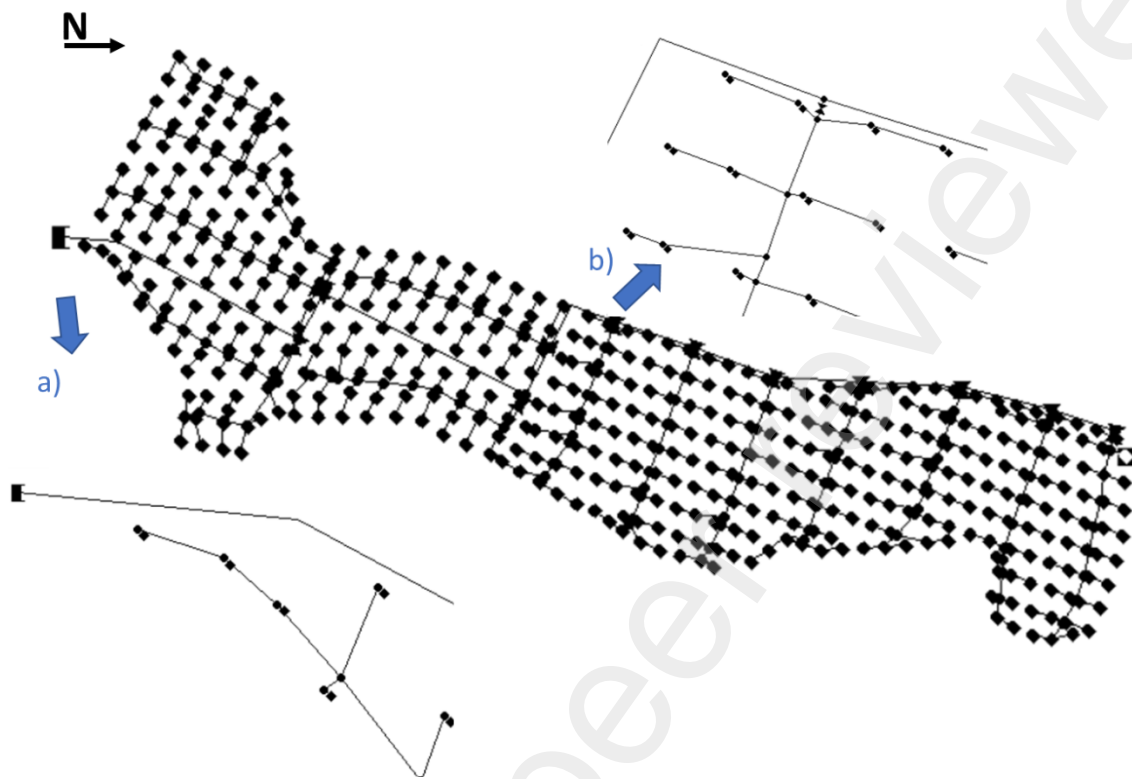
383 Two commercial solid-sets were characterized to demonstrate the model  
384 capacities: the CA solid-set, located in Castejón del Puente (Huesca, Spain), and  
385 the ZA solid-set, located in Monzón (Huesca, Spain). As built construction plans  
386 were available for both solid-set fields, which were used to create the required  
387 EPANET files and the solid-set information used to run the model. This information  
388 was treated in QGIS (QGIS Development Team, 2023) to analyze information and to  
389 create thematic maps of the solid-sets. Figures 3 and 4 present the maps of the CA  
390 and ZA solid-sets, respectively, as outlined in EPANET.

391 CA is a 10.2 ha plot with an elevation difference of 25.5 m, irrigated from one  
392 hydrant located at the lowest part of the field. It is equipped with 315 full-circle VYR  
393 36 sprinklers and 120 partial-circle VYR 66 sprinklers (28% of the sprinklers are  
394 partial-circle). The most common sprinkler spacing is triangular 18 x 18 m,  
395 although in the most elevated areas the spacing is triangular 15 x 18 (sprinklers  
396 separated 15 m within the line). The total number of sprinklers is 435, 43 sprinklers  
397 ha<sup>-1</sup>. The field has 12 sectors (from sector 13 to sector 24). The number of pipelines  
398 is 999. The total length of the pipelines is 9.2 km, or 0,90 km ha<sup>-1</sup>.

399 ZA is a 24.5 ha plot with an elevation difference of 17.1 m, irrigated from two  
400 hydrants (hydrant 1, 19,5 ha; hydrant 2, 5.0 ha) located at an intermediate elevation.  
401 It is equipped with 704 full-circle NDJ 5035 sprinklers and 195 partial-circle NDJ  
402 5035SD sprinklers (22% of the sprinklers are partial-circle). The most common  
403 sprinkler spacing is triangular 18 x 18 m, although in the most elevated areas the  
404 spacing is triangular 18 x 15 (sprinkler lines separated 15 m). The total number of  
405 sprinklers is 899, 37 sprinklers ha<sup>-1</sup>. The field has 26 sectors (sectors 1 to 6  
406 irrigated from hydrant 2; sectors 7 to 26 irrigated from hydrant 1). The number of  
407 pipelines is 2,024. The total length of the pipelines is 20.2 km, or 0.82 km ha<sup>-1</sup>.

408 Both solid-sets were built using a similar technique. The main pipes, extending  
409 from the hydrant to the valve of each sector, and the distribution pipelines within  
410 each sector were manufactured in PVC plastic using internal diameters from 59.2  
411 to 188.2 mm. Sprinkler lines were generally manufactured in 1" Polyethylene, with

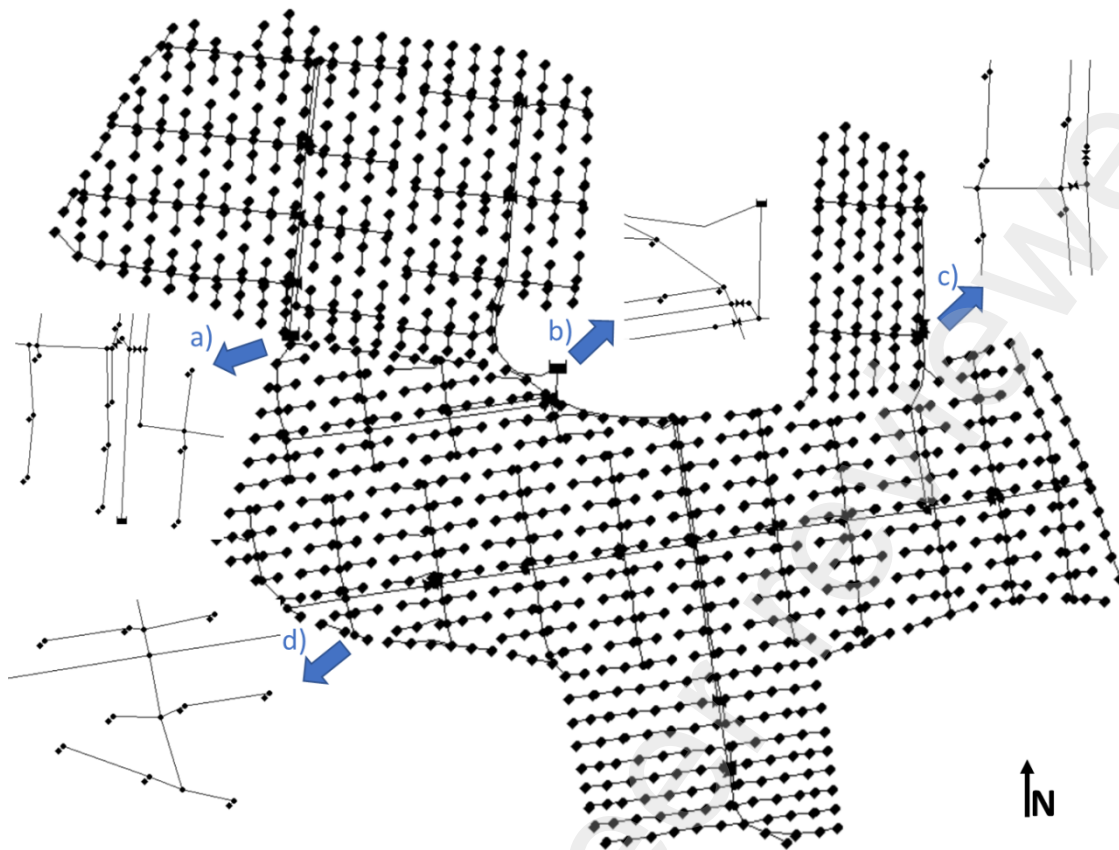
412 an internal diameter of 28 mm. Sprinkler risers were manufactured in galvanized  
 413 iron, with an internal diameter of 22 mm.



414

415 **Figure 3.** *EPANET layout of the CA solid-set field, with an irrigated area of 10.2 ha.*  
 416 *A hydrant sequentially irrigates 12 sectors (one sector at a time). Two details are*  
 417 *presented: a) the hydrant area; and b) the upstream part of sector 19 with its valve.*





418

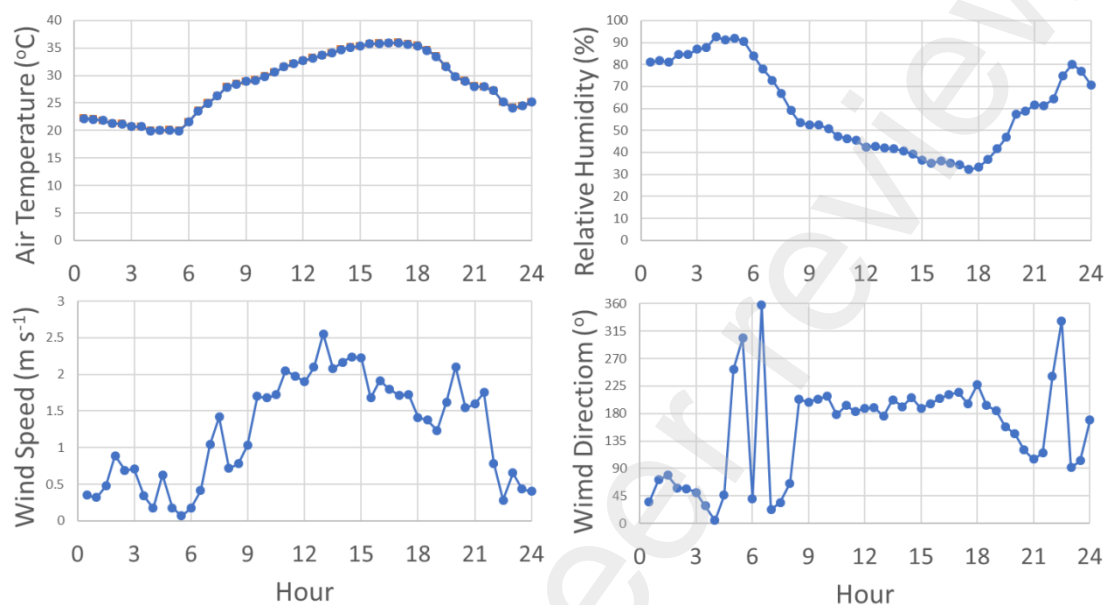
419 **Figure 4.** *EPANET layout of the ZA solid-set field, with an irrigated area of 24.5 ha.*  
 420 *Two hydrants irrigate 5.0 and 19.5 ha. The first hydrant sequentially irrigates 6*  
 421 *sectors, while the second hydrant sequentially irrigates 10 pairs of sectors (26*  
 422 *sectors in total; up to three sectors at a time). Four details are presented: a)*  
 423 *hydrant 2; b) hydrant 1; c) the valves of sectors 25 and 26; and d) pipelines*  
 424 *connecting sprinklers in sector 12.*

425 Square computational cells with a size of 3.6 x 3.6 m were created in both solid-  
 426 sets to accumulate irrigation water. A triangular 18 x 18 m sprinkler spacing fits 25  
 427 of these cells, the same number as catch cans in the experimental solid-sets. A  
 428 total of 8,333 and 18,809 cells were created in CA and ZA, respectively. These cells  
 429 are of types "internal" and "internal boundary". The other two types of  
 430 computational cells are automatically created by Ador-Sprinkler as needed.

### 431 2.7. Meteorological data

432 The commercial solid-sets are close to each other and to the nearest SiAR  
 433 agrometeorological station: Selgua (Huesca). The data set for 2022 was used for  
 434 simulation in CA and ZA, scheduling irrigation on August 1<sup>st</sup> (DOY 213). Figure 5  
 435 presents a plot of the key agrometeorological variables in that day: air

436 temperature, relative humidity, wind speed and wind direction. August 1<sup>st</sup> was a hot  
 437 and dry day with moderate winds during the day time and low winds during the  
 438 night time. Moderate winds blew from the south, while low winds blew from the  
 439 north.



440

441 **Figure 5.** *Semi hourly evolution of air temperature (°C), relative humidity (%), wind*  
 442 *speed (m s<sup>-1</sup>) and wind direction (°) on August 1<sup>st</sup> 2022 (DOY 213) at the Selgua*  
 443 *(Huesca, Spain) agro meteorological station.*

#### 444 2.8. Scheduling irrigation

445 Irrigation can be scheduled in Ador-Solid-Set using a tool similar to commercial  
 446 irrigation controllers. A number of irrigation programs can be created. Each  
 447 program is characterized by a starting date and a final date, an interval (days)  
 448 between program activations, the time of program start and a number of  
 449 sequentially irrigated subprograms. Each subprogram can irrigate a number of  
 450 field sectors for a number of minutes. When programs are intersected with the  
 451 half-hour periods of meteorological information, subperiods can be created. Each  
 452 subperiod has constant meteorological information and its duration is equal to or  
 453 less than half hour. A given subprogram can be composed of a number of  
 454 subperiods covering several half-hour intervals. Every subperiod is simulated  
 455 with the ballistic routine. An irrigation event is created by the execution of an  
 456 instance of a program. It involves one execution of all subperiods in each

457 subprogram. The addition of the irrigation depth applied to every computational  
458 cell in all subperiods is the irrigation depth resulting from the irrigation event.

Preprint not peer reviewed

459 The August 1<sup>st</sup> irrigation event was scheduled in the following way:

- 460 • CA
  - 461 ○ Program 1
    - 462 ▪ Starting at 0:00, ending at 24:00
    - 463 ▪ Sequential irrigation of all sectors: from 13 to 24, 120 minutes
    - 464 each.
  - 465 • ZA
    - 466 ○ Program 1
      - 467 ▪ Starting at 0:00, ending at 12:00
      - 468 ▪ Sequential irrigation of sectors 1 to 6. 120 minutes each
    - 469 ○ Program 2
      - 470 ▪ Starting at 4:00, ending at 24:00
      - 471 ▪ Sequential irrigation of sectors 9, 8, 7, 10, 11, 13, 12, 14, 15 and 16.
      - 472 120 minutes each
    - 473 ○ Program 3
      - 474 ▪ Starting at 4:00, ending at 24:00
      - 475 ▪ Sequential irrigation of sectors 19, 26, 18, 25, 24, 23, 17, 22, 21
      - 476 and 20. 120 minutes each

477 At the end of the day, all sectors have been irrigated for 120 min. The order of the  
 478 sectors in programs 2 and 3 is dictated by the need to make the most of hydraulic  
 479 energy. Program 2 irrigates sectors with high pressure (about 300 kPa), while  
 480 program 3 irrigates sectors with low pressure (200-300 kPa). The coincidence in  
 481 time of one sector from program 2 and another one from program 3 guarantees  
 482 sufficient pressure in all cases. The order of the sectors also ensures that key  
 483 pipelines are only used to irrigate one sector at a time, thus minimizing head  
 484 losses.

## 485 **2.9. Estimating roughness in the commercial solid-set fields**

486 Gao (2017) presented a methodology for the estimation of roughness in hydraulic  
 487 networks by using EPANET and minimizing the error in nodal pressure resulting  
 488 from roughness estimates. A similar approach was used in this research,  
 489 searching for the parameters that adequately parametrize EPANET to the

490 characteristics of the CA and ZA solid-sets. The key parameter is the roughness of  
 491 the different pipes. The Darcy-Weisbach roughness equation was selected, and  
 492 experiments were performed to calibrate its parameter  $\varepsilon$ (mm).

493 Experiments were performed by simultaneously measuring pressure with  
 494 calibrated manometers at two points of each pressurized network (1 network in  
 495 CA, 2 networks in ZA): just downstream of the hydrant and at a sprinkler. All  
 496 measurements were performed at maximum network pressure and 50 kPa below  
 497 maximum pressure. A distal sprinkler of each sector (far downstream from the  
 498 main pipes) was selected to characterize head losses when irrigating only this  
 499 sector. Additionally, a proximal sprinkler (near the main pipelines) was selected  
 500 to characterize head losses in the main pipelines. In CA, two sectors (13 and 14,  
 501 located furthest from the hydrant) were open to characterize the main pipelines.  
 502 In ZA, only sector 5 was open to characterize the main pipes of hydrant 2; two  
 503 sectors were open to characterize the main pipes of hydrant 1 (12 / 13 and 23 / 24).  
 504 As a result of these operations, 26 pairs of pressure observations were available  
 505 for CA and 58 pairs of pressure observations were available for ZA.

506 A specific software (CaliNet) was written in C++ to determine the value of the  
 507 objective function (O) in each solid-set field using EPANET simulations. The value  
 508 depends on the tested value of the roughness parameter in each pipe ( $\varepsilon_i$ ):

$$509 \quad O(\varepsilon_1, \varepsilon_2 \dots \varepsilon_n) = \frac{\sum_{i=1}^{i=n} (P_M - P_S)^2}{n} \quad [2]$$

510 Where n is the number of pipes and P is the pressure, which can be measured (M)  
 511 or simulated (S) with EPANET using the hypothesis of the roughness parameters.  
 512 The objective function is an error function. CaliNet was coupled to MPCOTool to  
 513 obtain optimum values of  $\varepsilon$  for each pipeline. Seven hypotheses were explored  
 514 regarding the values of  $\varepsilon$ :

- 515 • All pipelines in a network have the same roughness (1 parameter)
- 516 • There is a value for plastic pipes and another one for galvanized iron  
 517 pipelines (2 parameters)
- 518 • There is a value for PVC pipes, another one for polyethylene pipes and  
 519 another one for galvanized iron risers (3 parameters)

- 520 • There is a value for the main pipe, another one for all sectors and another  
521 one for galvanized iron risers (3 parameters)
- 522 • There is a value for the main pipe, another one each zone and another one  
523 for galvanized iron risers (5 parameters in CA, 7 parameters in ZA)
- 524 • There is a value for each pipeline diameter (10 parameters)
- 525 • There is a value for the main pipe, a value for each sector and a value for  
526 galvanized iron risers (14 parameters in CA, 28 parameters in ZA)

527 All hypotheses were tested in the search for the minimum value of the objective  
528 function in both solid-sets. In all cases, a minimum value of  $\epsilon$  was set to 0.0015 mm,  
529 corresponding to plastic materials. This prevented unrealistic low values of  
530 roughness, even negative values.

### 531 2.10. Mapping water application and estimating irrigation performance

532 QGIS was used to map water application resulting from the simulated irrigation  
533 event in CA and ZA. The Coefficient of uniformity was used to characterize  
534 irrigation performance in each sector. The values of additional drift were analysed.

## 535 3. Results and discussions

### 536 3.1. Determination of ballistic sprinkler parameters

537 Tables 2 and 3 present the optimum irrigation parameters for each sprinkler  
538 model and operating pressure. Parameters  $K_1$  and  $K_2$  also depend on wind speed,  
539 starting from zero at zero wind speeds. Ador Sprinkler linearly interpolates all  
540 parameters for intermediate values of pressure and - if needed - wind speed  
541 (Playán et al., 2006).

542  
543**Table 2.** Calibration parameters of the VYR sprinklers (full-circle and partial-circle models).

Model	Pressure (kPa)	D <sub>50</sub> (mm)	n	Wind m s <sup>-1</sup>	K <sub>1</sub>	K <sub>2</sub>
VYR36. Full-circle. 4.4 and 2.4 mm nozzles	200	2.74	1.11	0.00	0.000	0.000
				1.79	1.164	0.899
				2.29	0.180	0.982
				3.88	0.175	0.967
	300	1.72	1.61	0.00	0.000	0.000
				1.36	0.022	0.150
				3.55	0.027	0.875
				0.00	0.000	0.000
	400	1.69	1.61	0.48	0.157	0.130
				3.23	0.146	0.839
				0.00	0.000	0.000
				1.28	0.233	0.070
VYR66. Partial-circle. 4.0 and 2.4 mm nozzles	200	2.04	1.43	4.50	0.074	0.735
				0.00	0.000	0.000
				1.37	0.020	0.048
				3.61	0.233	0.342
	300	1.58	1.73	0.00	0.000	0.000
				1.15	0.161	0.137
				3.51	0.034	0.522
				0.00	0.000	0.000
400	1.44	1.88	1.15	0.161	0.137	
			3.51	0.034	0.522	

544

545 **Table 3.** Calibration parameters of the NDJ sprinklers (full-circle and partial-  
 546 circle models). Full-circle results were obtained by Paniagua (2016).

Model	Pressure kPa	D <sub>50</sub> mm	n	Wind m s <sup>-1</sup>	K <sub>1</sub>	K <sub>2</sub>
NDJ 5035. Full-circle. 4.5 and 2.5 mm nozzles	170	2.13	1.78	0.00	0.000	0.000
				0.74	0.076	0.117
				1.67	0.376	0.228
				2.67	0.209	0.139
	190	2.17	1.80	0.00	0.000	0.000
				0.88	0.644	0.132
				1.93	0.506	0.164
				2.75	0.179	0.242
	210	1.98	1.89	3.32	0.354	0.431
				0.00	0.000	0.000
				1.24	0.070	0.057
				1.91	0.351	0.096
300	1.79	2.03	3.39	0.327	0.256	
			0.00	0.000	0.000	
			1.28	0.623	0.117	
			1.97	0.829	0.144	
NDJ 5035SD. Partial- circle. 4.0 mm nozzle	200	2.10	1.95	2.74	0.192	0.111
				0.00	0.000	0.000
	300	1.82	2.17	1.77	0.260	0.064
				4.08	0.061	0.263
	400	1.62	2.30	0.00	0.000	0.000
				1.38	0.239	0.130
			4.34	0.374	0.131	
			0.00	0.000	0.000	
			1.67	0.442	0.057	
			2.93	0.527	0.048	

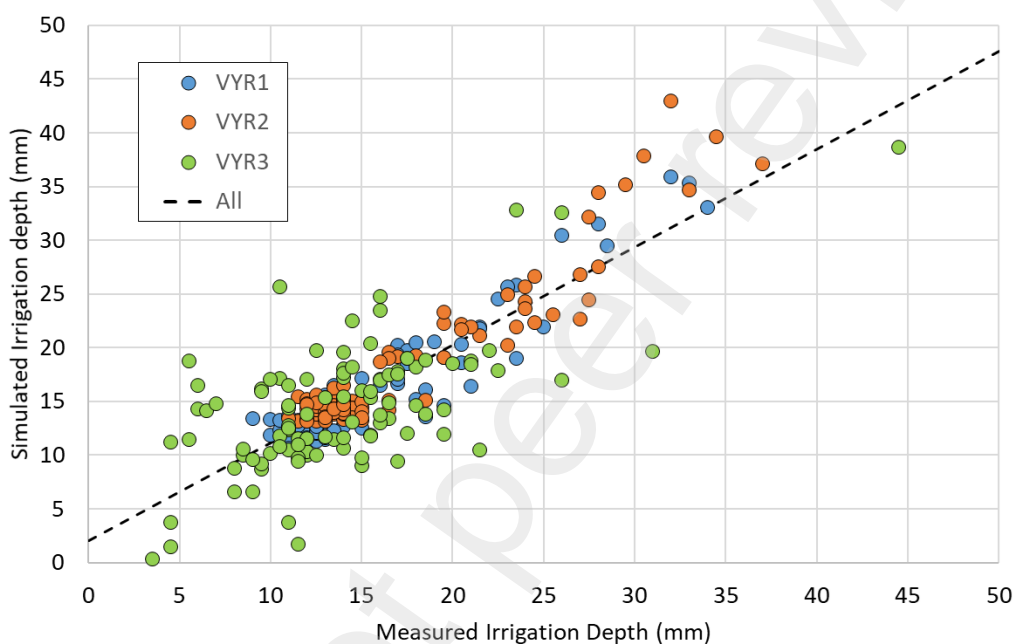
547

### 548 3.2. Validation of the ballistic model in the experimental solid-set

549 Measured and simulated irrigation depth in the catch cans are presented in Figure  
 550 6 as a scatter plot. The regression line was  $y = 0.911x + 2.01$ , with  $R^2 = 0.73^{***}$ . The  
 551 largest scatter was observed for experiment VYR3, the windiest of the series. In  
 552 the local conditions, strong winds also showed high variability in speed and  
 553 direction, which may not have been sufficiently revealed by the 30-minute

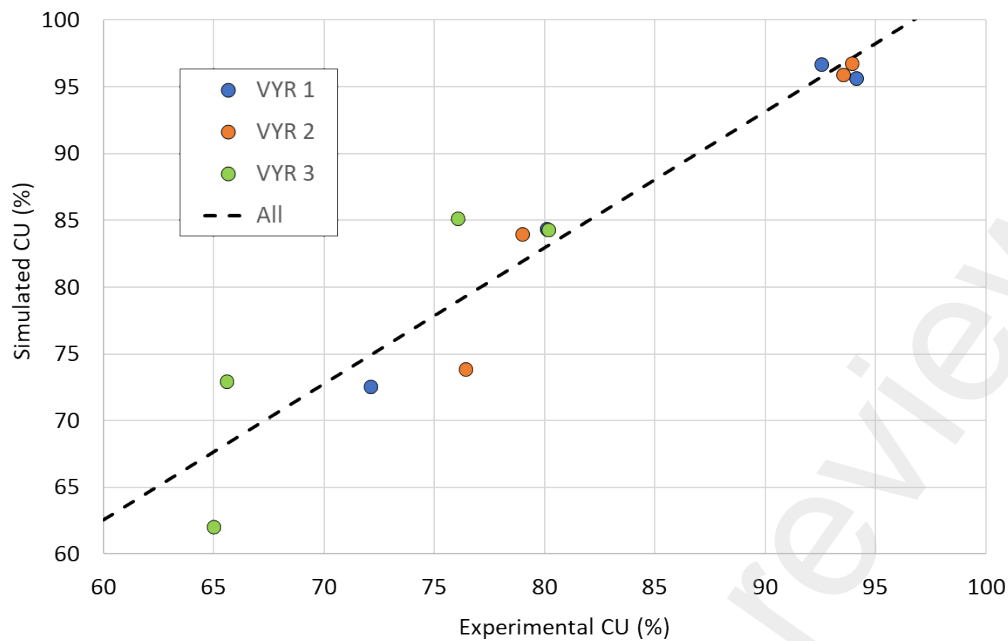


554 averages. The large range in irrigation depth (roughly between 0 and 45 mm) is  
 555 indicative of the existing variability. As a result, the values for CU were often low  
 556 (Figure 7), particularly in the sprinkler spacings including partial-circle  
 557 sprinklers. In experiments VYR1 and VYR2, with low and moderate winds,  
 558 uniformity was close to 95%, while in VYR3 uniformity dropped to 65% in the  
 559 sprinkler spacing with a 90° partial-circle sprinkler. The regression equation was  
 560  $y = 0.887x + 6.55$ , with  $R^2 = 0.89^{***}$ .



561

562 **Figure 6.** *Measured vs. simulated irrigation depth in the three solid-set*  
 563 *experiments.*



564

565 **Figure 7.** *Measured vs. simulated Coefficient of Uniformity in the four sprinkler*  
 566 *spacings of the three solid-set experiments.*

### 567 3.3. Determination of pipeline roughness in the commercial solid-set fields

568 Results of the roughness optimization process are presented in Table 4. The first  
 569 consideration is that the most complex model obtained the lowest values of error  
 570 in both solid-sets. Consequently, a roughness parameter was used for the main  
 571 pipes, another one for each sector and another for the sprinkler risers. This  
 572 approach led to 14 parameters in CA and 28 in ZA. Optimizing these parameters  
 573 required more than a million EPANET executions in each solid-set. The value of the  
 574 error function was always higher in ZA than in CA, suggesting the ZA had more  
 575 unexplained variability in observed pressure than CA. In fact, the collective  
 576 pressurized network supplying water to ZA has a construction problem in the  
 577 main pipeline (900 mm in diameter), and has had numerous fractures in the last  
 578 years, resulting in mud and small gravel often flowing into the solid-set pipelines.  
 579 The optimum value of the roughness parameters confirms that CA showed less  
 580 roughness than ZA, with average  $\varepsilon$  values of 0.379 and 1.33 mm, respectively.  
 581 Roughness was also less spatially variable in CA than in ZA, with standard  
 582 deviations of 0.421 and 1.23 mm, respectively. From the optimization point of view,  
 583 we did not expect that the most complex model would be selected. Such a complex  
 584 model can adapt very well to the spatial variability in roughness, but we could not

585 anticipate that the optimization tool would be able to identify such a large number  
586 of parameters, equal to half of the number of pairs of pressure observations.

587 **Table 4.** Calibration of pipeline roughness in the commercial solid-set fields.  
 588 Results of the seven calibration modes ordered by increasing error in both solid-  
 589 set fields. The number of calibrated parameters ( $n$ ) and the number of simulations  
 590 are presented in all cases.

CA Solid-Set Field				ZA Solid-Set Field			
Calibration mode	$n$	Error (kPa) <sup>2</sup>	Simulations	Calibration mode	$n$	Error (kPa) <sup>2</sup>	Simulations
Main / each sector / iron	14	34	1,081,344	Main / each sector / iron	2 8	202	1,048,576
Main / each zone / iron	5	88	74,240	Pipe diameters	10	357	524,288
Pipe diameters	10	114	734,600	Main / each zone / iron	7	419	296,960
Main / all sectors / Iron	3	143	19,096	PVC / PE / iron	3	523	19,096
Materials	2	149	4,704	Main / all sectors / iron	3	568	19,096
PVC / PE / Iron	3	149	19,096	Materials	2	619	4,704
All pipelines	1	192	712	All pipelines	1	619	712

591

592 **Table 5.** Calibration of pipeline roughness in the commercial solid-set fields.  
 593 Estimated value of Darcy-Weisbach  $\epsilon$  (mm) for the main pipeline, each sector and  
 594 the iron pipelines.

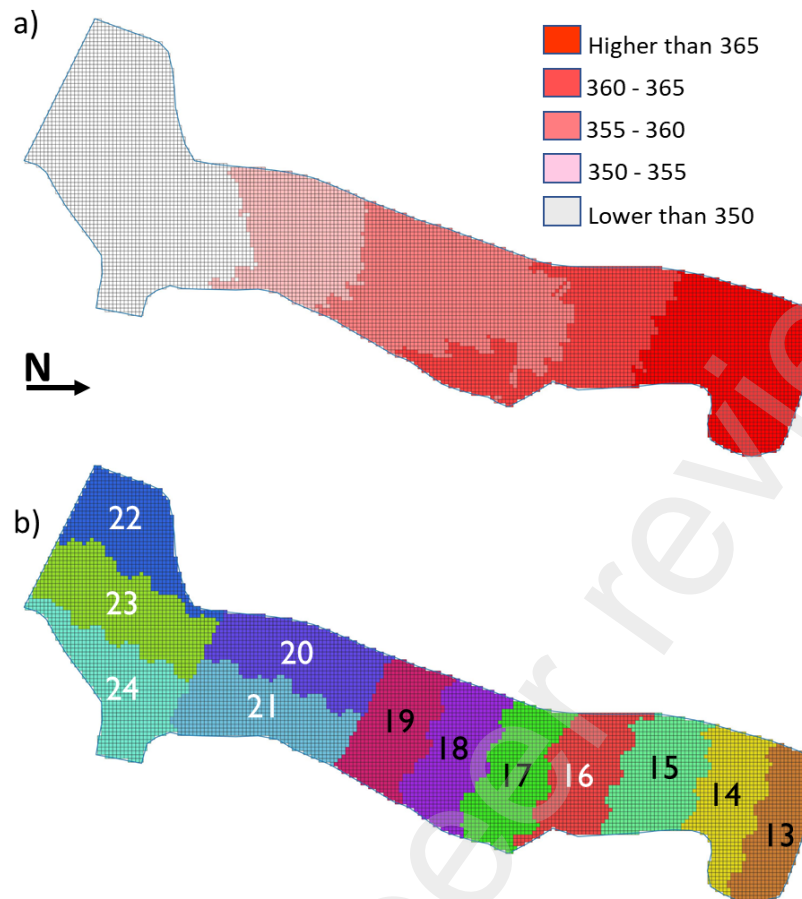
CA Solid-Set Field		ZA Solid-Set Field			
Pipelines	$\epsilon$ (mm)	Pipelines	$\epsilon$ (mm)	Pipelines	$\epsilon$ (mm)
Main	0.0015	Main	1.233	Sector 14	0.043
Sector 13	0.363	Sector 1	0.987	Sector 15	1.130
Sector 14	1.072	Sector 2	0.353	Sector 16	2.117
Sector 15	0.834	Sector 3	0.102	Sector 17	1.904
Sector 16	1.027	Sector 4	0.422	Sector 18	3.957
Sector 17	0.946	Sector 5	0.094	Sector 19	2.839
Sector 18	0.138	Sector 6	2.498	Sector 20	0.553
Sector 19	0.565	Sector 7	0.317	Sector 21	0.276
Sector 20	0.209	Sector 8	0.186	Sector 22	0.654
Sector 21	0.0015	Sector 9	2.886	Sector 23	1.181
Sector 22	0.048	Sector 10	0.353	Sector 24	5.147
Sector 23	0.0015	Sector 11	0.415	Sector 25	2.308
Sector 24	0.042	Sector 12	0.236	Sector 26	3.988
Iron	0.060	Sector 13	0.002	Iron	1.136

595

### 596 3.4. Simulation of an irrigation event in the commercial solid-set fields

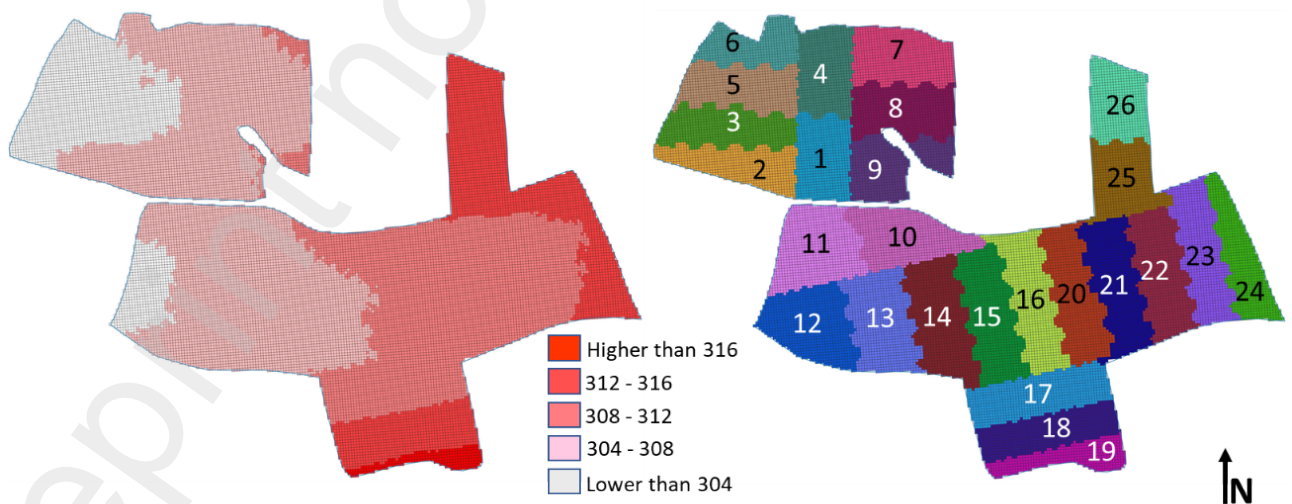
597 GIS processing of the information contained in the built solid-set projects  
598 permitted to prepare maps of soil surface elevation and irrigation sector for each  
599 computational cell. These maps are presented for CA and ZA in figures 8 and 9,  
600 respectively. The nearest sprinkler was attributed to each computational cell,  
601 creating a meandering effect on the sector boundaries.

602 EPANET files were prepared for each solid-set. This was a labor intense process,  
603 facilitated by importing nodal coordinates from the as built CAD solid-set map  
604 files. Pipelines were buried at 0.80 m, and risers set the sprinkler elevation at 2.20  
605 m. Figures 3 and 4 present some details of the solid-set characterization in  
606 EPANET, including hydrants, valves and pipeline connections. Pressure  
607 downstream from the CA Hydrant was 438 kPa. In ZA, pressure downstream from  
608 Hydrant 1 was 305 kPa, while pressure downstream from Hydrant 2 was 311 kPa.  
609 These pressures are low, particularly considering the differences in elevation in  
610 both solid-sets. Sprinklers in the high spots of both fields often operated at  
611 pressures lower than 200 kPa.



612

613 **Figure 8.** a) *Soil surface elevation above mean sea level (m); and b) irrigation*  
 614 *sectors in the CA solid-set field. The plots represent these variables in the*  
 615 *computational cells (3.6 x 3.6 m). The total difference in elevation is 25.5 m.*



616

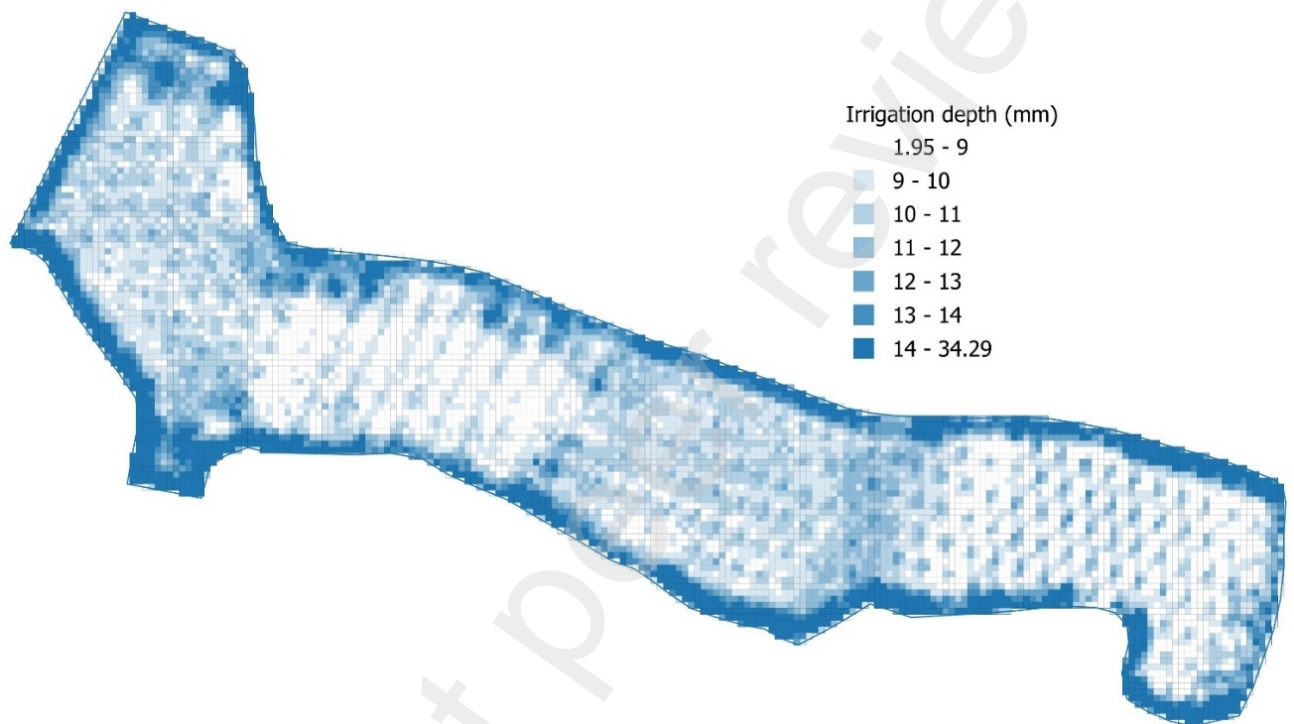
617 **Figure 9.** a) *Soil surface elevation above mean sea level (m); and b) irrigation*  
 618 *sectors in the ZA solid-set field. The plots represent these variables in the*  
 619 *computational cells (3.6 x 3.6 m). The total difference in elevation is 17.1 m.*

620 Figures 10 and 11 present the results of applying the irrigation schedule to the  
621 solid-set layout and the cell geometry for CA and ZA, respectively. Both figures  
622 show over irrigation at the boundaries, resulting from the large nozzle set of the  
623 partial-circle sprinklers when irrigating about 180° (the most common  
624 arrangement). When these sprinklers irrigate about 90° in corners, over irrigation  
625 is twice as intense.

626 Uniformity in CA was comparatively low in sectors 13 to 16 (Table 6, CU of 76–81%),  
627 where pressure is very low due to the high elevation and the long distance to the  
628 hydrant (although sprinkler spacing along the lines was reduced to 15 m in sectors  
629 13 to 19). As irrigation progressed downhill, uniformity increased. In sectors 20 to  
630 22, uniformity decreased due to the increased wind and to the accumulation of  
631 irrigation water in specific areas where sprinklers are too close. The evolution of  
632 WDEL along the day responded to the evolution of meteorological variables.  
633 Additional drift showed peak values in sectors 14 and 22. In both cases, the wind  
634 blew water out of the field: wind from the north blew water through the east side of  
635 sector 14, while wind from the south blew water through the west side of sector 22.  
636 The combination of local geometry and dominant winds determines the incidence  
637 of additional drift. Adding WDEL and additional drift, total WDEL reached a  
638 maximum value at sector 22 (24%). However, the CA average values were 13% for  
639 WDEL, 2.6% for additional drift and 16 for total WDEL. The whole-field CU was 81%,  
640 a value that is reasonable for field crops (Cuenca, 1989). However, this CU value  
641 corresponds to a complete solid-set, with wide pressure variations among  
642 sectors, meteorology variation along the day and different types of sprinklers. We  
643 do not believe that the threshold indicated by Cuenca (1989) can be readily applied  
644 to such a complex uniformity estimate.

645 The amount of water applied in ZA (Figure 11) followed the differences in soil  
646 surface elevation. The design of the highest sectors (18, 19, 25 and 26) reduced the  
647 distance between sprinkler lines, increasing water application. The amount of  
648 water applied by partial-circle sprinklers was not as different from that of full-  
649 circle sprinklers as it was in CA. In fact, nozzle diameters were smaller in ZA than  
650 in CA partial-circle sprinklers. Since there were up to three sectors irrigating at  
651 the same time, it is difficult to individualize the effect of meteorology on sector

652 performance. Additional drift in ZA (Table 7) was maximum between 10 and 12 h  
653 (5.10%). The wind from the south blew water through the north side of sectors 6 and  
654 10. Total WDEL reached its maximum value in this period (21.46%). The ZA average  
655 values were 12.06% for WDEL, 1.54% for additional drift and 13.61 for total WDEL. The  
656 whole-field CU was 81.01%

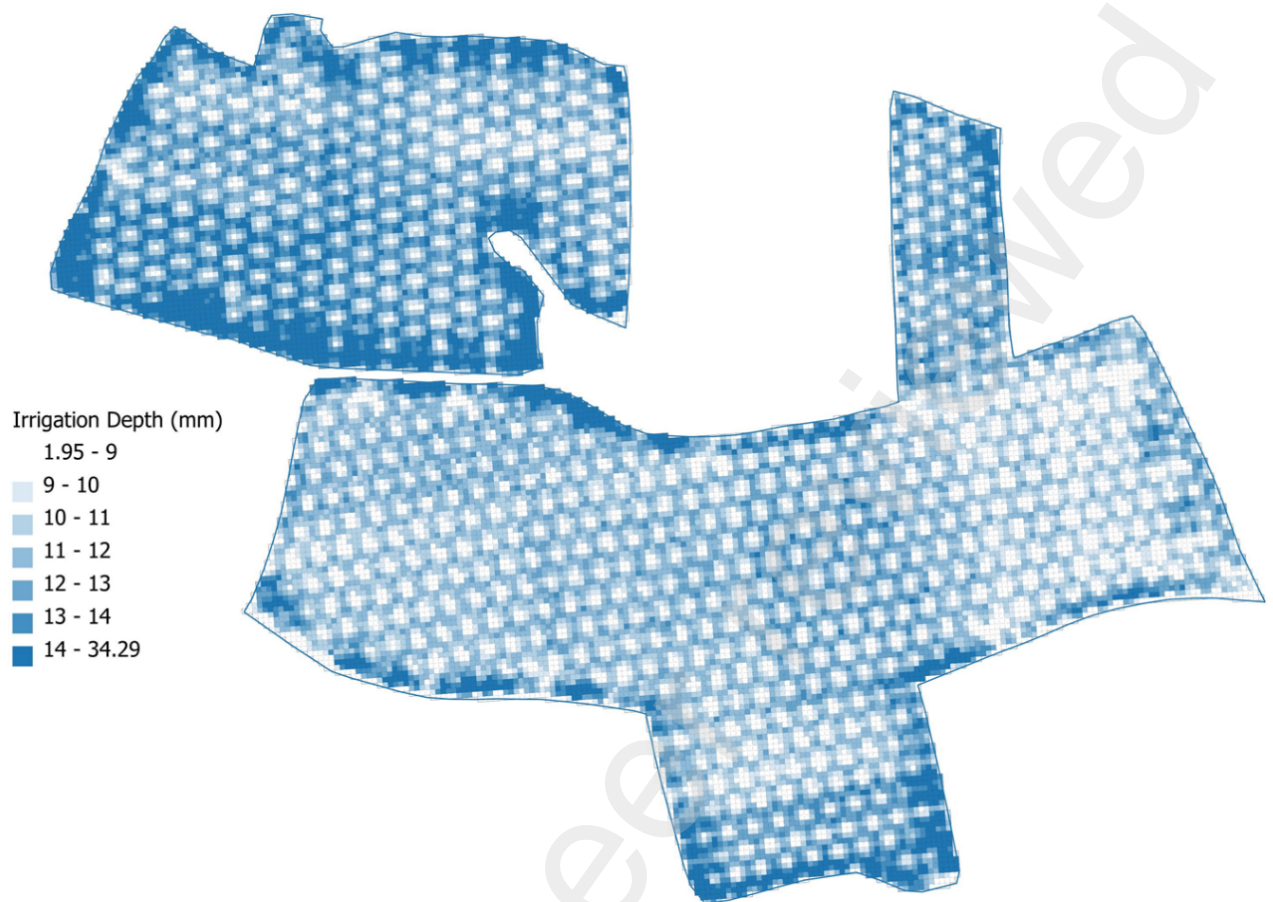


657

658

**Figure 10.** *Map of water application in the CA solid-set field.*





659

660

**Figure 11.** *Map of water application in the ZA solid-set field.*

661 **Table 6.** *Irrigation performance indicators in CA. The following variables are*  
 662 *presented for each 2-hour period: irrigating sector, CU, WDEL, additional drift and*  
 663 *total WDEL.*

Hour	Sector irrigating	CU	WDEL	Additional Drift	Total WDEL
-	-	%	%	%	%
0-2	13	78.22	7.86	2.19	10.05
2-4	14	76.54	6.64	5.07	11.71
4-6	15	81.43	5.78	1.71	7.49
6-8	16	80.98	10.95	1.88	12.84
8-10	17	85.86	14.17	2.92	17.09
10-12	18	84.33	17.55	1.62	19.18
12-14	19	84.74	19.40	1.27	20.67
14-16	20	80.59	19.56	1.04	20.60
16-18	21	83.67	18.77	3.25	22.02
18-20	22	80.61	17.18	6.58	23.77
20-22	23	88.53	13.32	0.84	14.16
22-24	24	72.99	9.06	2.63	11.69

664

665 **Table 7.** *Irrigation performance indicators in ZA. The following variables are*  
 666 *presented for each 2-hour period: irrigating sector, CU, WDEL, additional drift and*  
 667 *total WDEL. Up to three sectors irrigate at the same time in this solid-set.*

Hour	Sector irrigating	CU	Sector irrigating	CU	Sector irrigating	CU	WDEL	Addition al Drift	Total WDEL
-	-	%	-	%	-	%	%	%	%
0-2	1	83.91					6.29	0.75	7.04
2-4	2	81.99					5.43	2.46	7.90
4-6	3	82.87	9	79.68	19	80.26	4.56	2.39	6.96
6-8	4	84.80	8	82.19	26	83.61	9.60	0.86	10.46
8-10	5	83.89	7	82.30	18	82.50	13.13	1.23	14.36
10-12	6	82.16	10	83.00	25	84.34	16.35	5.10	21.46
12-14			11	85.32	24	82.77	18.20	3.21	21.41
14-16			13	83.72	23	82.07	18.36	0.56	18.92
16-18			12	82.57	17	83.47	17.54	1.25	18.79
18-20			14	85.77	22	83.70	15.44	0.09	15.53
20-22			15	85.45	21	83.27	12.48	0.38	12.86
22-24			16	83.96	20	83.98	7.38	0.23	7.61

668

669 These simulations are exploratory in nature, and were designed to illustrate  
 670 model capacities. Local farmers try to avoid irrigation from noon to 8 pm,  
 671 increasing CU and decreasing WDEL. Additionally, scheduling irrigation by volume  
 672 would reduce differences in irrigation depth among sectors.

673 Simulating irrigation in large solid-sets requires a large computational effort,  
 674 particularly in the ballistic model. The Ador-Sprinkler library has been  
 675 parallelized to take advantage of the large number of computational threads  
 676 available in current personal computers. Running a seasonal simulation of ZA and  
 677 CA will take a few minutes. The coupled nature of the model permits to perform  
 678 unattended simulations once the solid-set and the sprinklers have been properly  
 679 characterized. This is an important feature if the model is used to explore solutions  
 680 or if it is run iteratively for optimization processes.

#### 681 4. Conclusions

682 Solid-set models permit to progress from performance estimates based on a few  
683 sprinklers to field-scale performance. Irrigation uniformity indicators derived at  
684 this scale are conceptually different from those focusing on a few sprinklers.  
685 Uniformity thresholds in the literature need to be assessed for adequacy to the  
686 field-scale. This responds to the use of different types of sprinklers and to the  
687 presence of relevant spatial variability in pressure and relevant time variability in  
688 meteorology. The interaction between full- and partial-circle sprinklers can be  
689 evaluated using this type of models. The adequate choice of partial-circle models  
690 and their nozzle packages seems to be a key requirement for field-scale  
691 uniformity. In the analyzed commercial solid-sets, partial-circle sprinklers  
692 applied much more water than full circle sprinklers, lowering uniformity and  
693 leading to reduced efficiency. The proposed model has revealed a new, additional  
694 drift term. Field-scale models permit to assess the water blown away from the  
695 irrigation domain at the field boundaries. This has a relatively small quantitative  
696 effect, but can be relevant in specific sector geometries and winds, as well as  
697 during fertigation events. EPANET has permitted running complex hydraulic  
698 analyses with minimum effort *via* programming. Unfortunately, characterizing  
699 commercial solid-sets in EPANET remains a time-consuming process. The model  
700 needs to extend its capacities to address challenges related to water quantity and  
701 quality. Optimizing seasonal irrigation programming, estimating irrigation  
702 efficiency / crop yield and minimizing non-point agricultural pollution through  
703 adequate irrigation and fertilization are key issues for future developments.  
704 Farmers require directions to make their production processes clean, sustainable  
705 and profitable.

706 **5. Declaration of Competing Interest**

707 The authors declare that they have no known competing financial interests or  
708 personal relationships that could have appeared to influence the work reported in  
709 this paper.

710 **6. Acknowledgement**

711 This research was funded through grants AGL2017-89407-R and PID2021-  
712 1240950B-I00 by MCIN/AEI/10.13039/501100011033 and by ERDF, a way of making  
713 Europe.

714 Thanks are due to César Romano (EEAD-CSIC), Miguel Izquierdo (CITA Aragón)  
715 and Vicente Villarroya (CITA Aragón) for their technical support.

716 **7. References**

- 717 Bassett, D., 1972. Mathematical-model of water advance in border irrigation. Trans  
718 ASAE 15, 992-.
- 719 Barberena, I., Campo-Bescós, M.Á., Casalí, J. 2022. Extended Assessment of  
720 Sprinkler Irrigation Uniformity in Greenhouses Using GIS and Hydraulic  
721 Modeling. Sustainability 14, 9723. <https://doi.org/10.3390/su14159723>
- 722 Bautista, E., Schlegel, J., 2020. Modeling Solute Transport in the WinSRFR Surface  
723 Irrigation Software. J Irrig Drain Eng 146. [https://doi.org/10.1061/\(ASCE\)IR.1943-4774.0001507](https://doi.org/10.1061/(ASCE)IR.1943-4774.0001507)
- 724
- 725 Burguete, J., Latorre, B., 2018. MPCOTool: The Multi-Purposes Calibration and  
726 Optimization Tool. GitHub, Spain. Github.
- 727 Carrión, P., Tarjuelo, J.M., Montero, J., 2001. SIRIAS: a simulation model for  
728 sprinkler irrigation: I. Description of the model. Irrig Sci 2001, 73–84.  
729 <https://doi.org/10.1007/s002710000031>
- 730 Christiansen, J.E., 1942. Irrigation by sprinkling (No. Bulletin 670). California  
731 Agricultural Experimental Station, University of California, Berkley, California,  
732 USA.
- 733 Cuenca, R.H., 1989. Irrigation system design: an engineering approach. Prentice-  
734 Hall, Inc., Englewood Cliffs, New Jersey.
- 735 de Andrade, C., Allen, R., 1999. SPRINKMOD - pressure and discharge simulation  
736 model for pressurized irrigation systems. 1. Model development and  
737 description. Irrig Sci 18, 141–148. <https://doi.org/10.1007/s002710050055>
- 738 de Andrade, C., Allen, R., Wells, R., 1999a. SPRINKMOD - pressure and discharge  
739 simulation model for pressurized irrigation systems. 2. Sensitivity to lateral  
740 hydraulic parameters and leakage. Irrig Sci 18, 157–161.  
741 <https://doi.org/10.1007/s002710050057>
- 742 de Andrade, C., Wells, R., Allen, R., 1999b. SPRINKMOD - pressure and discharge  
743 simulation model for pressurized irrigation systems. 2. Case study. Irrigation  
744 Sci 18, 149–156. <https://doi.org/10.1007/s002710050056>
- 745 Dechmi, F., Playán, E., Cavero, J., Martínez-Cob, A., Faci, J.M., 2004. A coupled crop  
746 and solid set sprinkler simulation model: I. Model development. J Irrig Drain Eng  
747 130, 499–510. [https://doi.org/10.1061/\(ASCE\)0733-9437\(2004\)130:6\(499\)](https://doi.org/10.1061/(ASCE)0733-9437(2004)130:6(499))
- 748 Dechmi, F., Playán, E., Faci, J.M., Tejero, M., Bercero, A., 2003. Analysis of an  
749 irrigation district in northeastern Spain: II: Irrigation evaluation, simulation and  
750 scheduling. Agric Water Manage 61, 93–109. [https://doi.org/10.1016/S0378-3774\(03\)00021-0](https://doi.org/10.1016/S0378-3774(03)00021-0)
- 751
- 752 Fukui, Y., Nakanishi, K., Okamura, S., 1980. Computer evaluation of sprinkler  
753 irrigation uniformity. Irrig Sci 2, 23–32. <https://doi.org/10.1007/BF00285427>
- 754 Gao, T. 2017. Pipe Roughness Estimation in Water Distribution Networks Using  
755 Head loss Adjustment. J Water Resour Plann Manage, -1--1. Paper 04017007.  
756 [http://dx.doi.org/10.1061/\(ASCE\)WR.1943-5452.0000752](http://dx.doi.org/10.1061/(ASCE)WR.1943-5452.0000752)
- 757 Jones, D., Snider, C., Nassehi, A., Yon, J., Hicks, B., 2020. Characterising the Digital  
758 twin: A systematic literature review. CIRP J Manuf Sci Technol 29, 36–52.  
759 <https://doi.org/10.1016/j.cirpj.2020.02.002>
- 760 Li, J., Kawano, H., Yu, K., 1994. Droplet size distributions from different shaped  
761 sprinkler nozzles. Trans ASAE 37, 1871–1878.

- 762 Montero, J., Tarjuelo, J.M., Carrión, P., 2001. SIRIAS: a simulation model for  
763 sprinkler irrigation: II. Calibration and validation of the model. *Irrig Sci* 2001, 85–  
764 98. <https://doi.org/10.1007/s002710000032>
- 765 Morcillo García, M., Moreno Hidalgo, M. Á., Ballesteros González, R., Montero  
766 Martínez, J., del Castillo Sánchez-Caamañes, A., 2021. Integración de modelos  
767 hidráulicos, de distribución de agua y de cultivo para el análisis holístico de  
768 sistemas de riego por aspersión fija. Presented at the XXXVIII Congreso  
769 Nacional de Riegos, Cartagena.
- 770 Ouazaa, S., Burguete, J., Zapata, N., 2016. Solid-set sprinklers irrigation of field  
771 boundaries: experiments and modeling. *Irrig Sci* 34, 85–103.  
772 <https://doi.org/10.1007/s00271-016-0492-x>
- 773 Ouazaa, S., Latorre, B., Burguete, J., Serreta, A., Playan, E., Salvador, R., Paniagua,  
774 P., Zapata, N., 2015. Effect of the start-stop cycle of center-pivot towers on  
775 irrigation performance: Experiments and simulations. *Agric Water Manage* 147,  
776 163–174. <https://doi.org/10.1016/j.agwat.2014.05.013>
- 777 Paniagua, M.P., 2016. Mejora del riego por aspersión en parcela: caracterización de  
778 aspersores a baja presión, estudio de diferentes sistemas de medición de gotas  
779 y análisis del modelo balístico. (Doctoral thesis). University of Zaragoza,  
780 Zaragoza, Spain. In Spanish.
- 781 Pereira, L., Douieb, A., Bounoua, R., Lamaddalena, N., Sousa, P., 1998. Model for  
782 design of low pressure distribution irrigation systems, in: Zazueta, F., Xin, J.  
783 (Eds.), *Universidade de Lisboa. Presented Computers in Agriculture*, 1998, pp.  
784 183–191.
- 785 Playán, E., Slatni, A., Castillo, R., Faci, J.M., 2000. A case study for irrigation  
786 modernisation: II. Scenario Analysis. *Agric Water Manage* 42, 335–354.  
787 [https://doi.org/10.1016/S0378-3774\(99\)00051-7](https://doi.org/10.1016/S0378-3774(99)00051-7)
- 788 Playán, E., Zapata, N., Faci, J.M., Tolosa, D., Lacueva, J.L., Pelegrín, J., Salvador, R.,  
789 Sánchez, I., Lafita, A., 2006. Assessing sprinkler irrigation uniformity using a  
790 ballistic simulation model. *Agric Water Manage* 84, 89–100.  
791 <https://doi.org/10.1016/j.agwat.2006.01.006>
- 792 Press, W. H., Flannery, B. P., Teukolsky, S. A., and Vetterling, W. T. 1988. *Numerical*  
793 *recipes in C*. Cambridge University Press. 735 pp,
- 794 QGIS Development Team, 2023. QGIS Geographic Information System. Open  
795 Source Geospatial Foundation Project.
- 796 Robles, O., Latorre, B., Zapata, N., Burguete, J., 2019. Self-calibrated ballistic model  
797 for sprinkler irrigation with a field experiments data base. *Agric Water Manage*  
798 223. <https://doi.org/10.1016/j.agwat.2019.105711>
- 799 Rossman, L.A., Clark, R.M., Grayman, W.M., 1994. Modeling chlorine residuals in  
800 drinking-water distribution-systems. *J Environ Eng* 120, 803–820.  
801 [https://doi.org/10.1061/\(ASCE\)0733-9372\(1994\)120:4\(803\)](https://doi.org/10.1061/(ASCE)0733-9372(1994)120:4(803))
- 802 Seginer, I., Nir, D., von Bernuth, D., 1991. Simulation of wind-distorted sprinkler  
803 patterns. *J Irrig Drain Eng* 117, 285–306. [https://doi.org/10.1061/\(ASCE\)0733-9437\(1991\)117:2\(285\)](https://doi.org/10.1061/(ASCE)0733-9437(1991)117:2(285))
- 804
- 805 Skaggs, T., Trout, T., Simunek, J., Shouse, P., 2004. Comparison of HYDRUS-2D  
806 simulations of drip irrigation with experimental observations. *J Irrig Drain Eng*  
807 130, 304–310. [https://doi.org/10.1061/\(ASCE\)0733-9437\(2004\)130:4\(304\)](https://doi.org/10.1061/(ASCE)0733-9437(2004)130:4(304))

- 808 Steduto, P., Hsiao, T., Raes, D., Fereres, E., 2009. AquaCrop-The FAO Crop Model to  
809 Simulate Yield Response to Water: I. Concepts and Underlying Principles. *Agron*  
810 *J* 101, 426–437. <https://doi.org/10.2134/agronj2008.0139s>
- 811 Tarjuelo, J.M., Carrión, P., Valiente, M., 1994. Simulación de la distribución del riego  
812 por aspersión en condiciones de viento. *Investigación Agraria: producción y*  
813 *protección vegetal* 9, 255–271. In Spanish.
- 814 Vories, E.D., D., von Bernuth.R., Mickelson, R.H., 1987. Simulating sprinkler  
815 performance in wind. *J Irrig Drain Eng* 113, 119–130.  
816 [https://doi.org/10.1061/\(ASCE\)0733-9437\(1987\)113:1\(119\)](https://doi.org/10.1061/(ASCE)0733-9437(1987)113:1(119))
- 817 Windsor, J., Chow, V., 1971. Optimization model of a farm irrigation system. *Trans*  
818 *Am Geophys Union* 52, 199–.
- 819 Wu, I., Gitlin, H., 1974. Drip irrigation design based on uniformity. *Trans ASAE* 17,  
820 429–432.
- 821 Zapata, N., Bahddou, S., Latorre, B., Playan, E., 2023. A simulation tool to optimize  
822 the management of modernized infrastructures in collective and on-farm  
823 irrigation systems. *Agric Water Manage* 284.  
824 <https://doi.org/10.1016/j.agwat.2023.108337>
- 825 Zapata, N., El Malki, E.H., Latorre, B., Gallinat, J., Citoler, F.J., Castillo, R., Playan, E.,  
826 2017. A simulation tool for advanced design and management of collective  
827 sprinkler-irrigated areas: a study case. *Irrig Sci* 35, 327–345.  
828 <https://doi.org/10.1007/s00271-017-0547-7>
- 829 Zapata, N., Playán, E., Faci, J.M., 2000. Water reuse in sequential basin irrigation. *J*  
830 *Irrig Drain Eng* 126, 362–370. [https://doi.org/10.1061/\(ASCE\)0733-9437\(2000\)126:6\(362\)](https://doi.org/10.1061/(ASCE)0733-9437(2000)126:6(362))  
831